

Attitude motion of cylindrical space debris during its removal by ion beam

Vladimir S. Aslanov¹, Alexander S. Ledkov²

¹Samara National Research University, 34, Moscovskoe shosse, Samara, 443086,
aslanov_vs@mail.ru, aslanov.ssau.ru

²Samara National Research University, 34, Moscovskoe shosse, Samara, 443086,
ledkov@inbox.ru, www.ledkov.com

Abstract

The paper is devoted to the problem of space debris mitigation. Non-contact method of the space debris deorbiting is considered. It is assumed that ion thrusters, which are installed on the active spacecraft, create the ion flow, that blows the debris and slow it down. The objectives of this work are development of mathematical models and research the space debris motion under the action of the ion flow. It is supposed that the space debris is a rigid body of a cylindrical shape. Calculation of ion beam force and torque was performed using Newton Impact theory. Mathematical models describing the spatial and plane motions of the cylindrical space debris under the influence of gravity gradient torque and the ion flux was constructed. It was showed that motion of the space debris around its center of mass has a significant effect on its removal time. For the case of plane motion, phase portraits describing the motion of the space debris relative its center of mass were constructed. Comparison of the descent times in different motion modes was carried out. The results can be used to create new effective systems of large space debris removal.

1. Introduction

In the last years in the scientific literature great attention has been paid to the problem of transportation of not functioning satellites and space debris removal. The majority of works were devoted to systems that imply a stage of docking or capturing a transported object by harpoons [1], a net [2], a tether [3], or by a robotic manipulator [4]. A detailed overview of the capture tools and methods is given in the work [5]. Docking with an unmanaged object is a complex technical task. Failure at this stage is highly probable and can lead to the formation of new debris. An alternative is the use of noncontact transportation methods: based on the Coulomb interaction [6] and on the ion beam created by the electric-reactive engine [7].

The use of ion beam involves the placement of electric-reactive engines on an active spacecraft. These engines are not something exotic and widely used in modern aerospace [8]. The engines "blow" on the transported object and thus change the parameters of its motion. To

date, "Ion Beam Shepherd" is best-designed project in this field. Existing studies show that the considered method allows to remove an object with a mass of several tons from the orbit with a height of the order of 1000 km for several months [7]. Works [9, 10] are devoted to the estimation of influence of the ion beam created by an electric-reactive engine, on objects of the various forms. There are studies in which the optimal control laws of the active spacecraft for the space debris removal from orbit are developed [11, 12]. Analysis of the literature shows that in existing studies due attention is not paid to the motion of the transported object relative to its center of mass. Meanwhile, part of the energy transferred by the ion flow can be spent on the spin up of the object, rather than braking.

The aims of this work are development of mathematical models and research space debris motion under the action of the ion flow. It is supposed that the space debris is a rigid body of a cylindrical shape.

2. Materials and Methods

Mathematical models of a space debris motion under the action of the gravitational moment and ion flux will be developed in this section for the general case and for the particular case of plane motion. Method of the ion beam resultant force and torque calculation will be also described.

2.1 Equations of motion

The attitude motion of the space debris is considered. It is assumed that the space debris is a rigid body; the Earth does not rotate and it has spherical shape; the active spacecraft, which creates ion flow, is maintained in a fixed position relative to the center of mass of the space debris by its control system. It is supposed that only gravitational and ion forces and torques act on the space debris.

Let us introduce coordinate systems. $Ox_p y_p z_p$ is inertial frame. Origin O is the center of the Earth. The plane $Ox_p z_p$ is equatorial, the axis Oy_p coincides with the axis of rotation of the Earth. The origin of the orbital frame $Cx_o y_o z_o$ is located at the center of mass of the space debris (Figure 1). The axis z_o lies along the radius vector \mathbf{r} of the center of mass. The axis x_o lies in the plane of the orbit and is directed towards the orbital flight. The axis y_o is perpendicular to the orbital plane. The body frame $Cx_b y_b z_b$ is fixed relative to the space debris. Its axes are not the principal body axes. Transformation from one reference frame to another can be defined by rotation matrices

$$\mathbf{M}_O^b = \begin{bmatrix} a_{11} & a_{12} & a_{13} \\ a_{21} & a_{22} & a_{23} \\ a_{31} & a_{32} & a_{33} \end{bmatrix},$$

$$\mathbf{M}_O^p = \begin{bmatrix} \cos \psi \cos \nu - \sin \psi \sin \lambda \sin \nu & \sin \psi \cos \lambda & -\cos \psi \sin \nu - \sin \psi \sin \lambda \cos \nu \\ -\sin \psi \cos \nu - \cos \psi \sin \lambda \sin \nu & \cos \psi \cos \lambda & \sin \psi \sin \nu - \cos \psi \sin \lambda \cos \nu \\ \cos \lambda \sin \nu & \sin \lambda & \cos \lambda \cos \nu \end{bmatrix}.$$

Here lower index denotes new frame, upper index denotes old frame: $\mathbf{x}_{new} = \mathbf{M}_{new}^{old} \mathbf{x}_{old}^T$, where \mathbf{x}_i is some vector given by the coordinates in i -th frame, \mathbf{M}_O^b is direction cosine matrix. Its elements a_{ij} are the cosines of the angles between i -th unit vector of the orbital frame and j -th unit vector of the body frame. Angles ν , λ , ψ specify the transition from frame $Ox_p y_p z_p$ to $Cx_o y_o z_o$ and are shown in Figure 1. The velocity vector \mathbf{V}_c of the space debris center of mass lies in the plane $Cx_o z_o$.

The active spacecraft is a material point B (Figure 1). Its radius vector has the following coordinates $\mathbf{p}_B = \overline{CB} = [\rho_B, 0, 0]^T$ in $Cx_o y_o z_o$ frame. The direction of the ion beam axis is defined by the angles α and β . Let us introduce coordinate frame $Bx_a y_a z_a$. The axis x_a is directed along ion beam axis to flight direction, z_a lies in the same plane with z_o axis. The axis y_a completes the right-handed set. Transformation from $Bx_o y_o z_o$ to $Bx_a y_a z_a$ can be defined by the matrix

$$\mathbf{M}_a^o = \begin{bmatrix} \cos \alpha \cos \beta & \cos \alpha \sin \beta & -\sin \alpha \\ -\sin \beta & \cos \beta & 0 \\ \sin \alpha \cos \beta & \sin \alpha \sin \beta & \cos \alpha \end{bmatrix}.$$

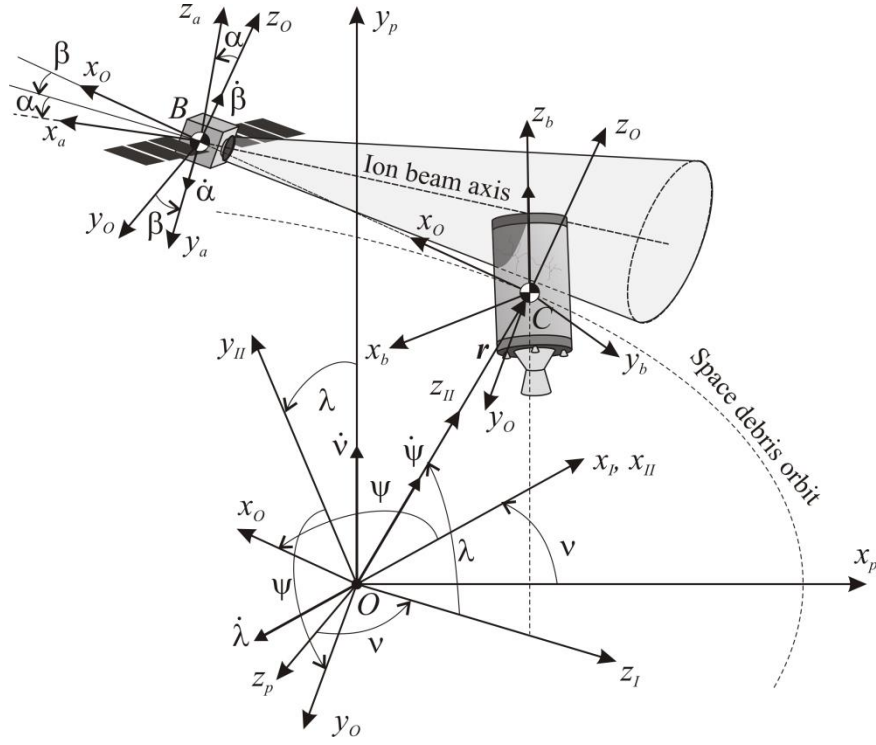


Figure 1: Coordinate frames.

The equations of the debris center of mass motion can be written in the form

$$m\mathbf{W} = \mathbf{G} + \mathbf{F}_I. \quad (1)$$

Here m is the mass of the space debris, $\mathbf{W} = \ddot{\mathbf{r}}$ is the acceleration of the point C, $\mathbf{r} = [r \cos \lambda \sin \nu, r \sin \lambda, r \cos \lambda \cos \nu]$ is the radius or the point C given in the inertial frame, $\mathbf{G} = -\frac{m\mu}{r^3}\mathbf{r}$ is the gravitational force, μ is the gravitational constant of the Earth, $\mathbf{F}_I = [F_{I_x}, F_{I_y}, F_{I_z}]$ is the ion beam force, which is specified in the orbital reference frame. Projecting equation (1) onto the axis of the inertial frame and expressing the second derivatives yields

$$\begin{aligned} \ddot{r} &= r(\dot{\nu}^2 \cos^2 \lambda + \dot{\lambda}^2) - \frac{\mu}{r^2} + \frac{F_{I_z}}{m}, \\ \ddot{\nu} &= 2\dot{\nu} \left(\dot{\lambda} \tan \lambda - \frac{\dot{r}}{r} \right) + \frac{F_{I_x} \cos \psi - F_{I_y} \sin \psi}{mr}, \\ \ddot{\lambda} &= -\dot{\nu}^2 \sin \lambda \cos \lambda - \frac{2\dot{r}\dot{\lambda}}{r} + \frac{F_{I_x} \sin \psi + F_{I_y} \cos \psi}{mr}. \end{aligned} \quad (2)$$

Euler rotational equations of the space debris motion can be written in the form [13]

$$[\mathbf{I}]\dot{\boldsymbol{\omega}} = -\boldsymbol{\omega} \times [\mathbf{I}]\boldsymbol{\omega} + \mathbf{L}_G + \mathbf{L}_I. \quad (3)$$

Here $\boldsymbol{\omega} = [\omega_x, \omega_y, \omega_z]$ is the instantaneous angular velocity vector of the body frame relative to the inertial frame in body frame components, \mathbf{L}_G is the gravity gradient torque vector relative

the space debris center of mass, \mathbf{L}_I is the ion beam torque vector relative the space debris center of mass, $[\mathbf{I}]$ is the inertia matrix

$$[\mathbf{I}] = \begin{bmatrix} I_x & -I_{xy} & -I_{xz} \\ -I_{xy} & I_y & -I_{yz} \\ -I_{xz} & -I_{yz} & I_z \end{bmatrix}.$$

In general case the gravity gradient torque vector \mathbf{L}_G can be written as [13]

$$\mathbf{L}_G = \frac{3\mu}{r^5} \mathbf{r} \times [\mathbf{I}] \mathbf{r}. \quad (4)$$

Vector \mathbf{r} in the body frame have the coordinates

$$\mathbf{r} = [a_{31}r, a_{32}r, a_{33}r]. \quad (5)$$

Let us write projections of the gravity gradient torque on the axes of body frame, taking into account (5)

$$\begin{aligned} L_{Gx} &= \frac{3\mu}{r^3} \left((I_z - I_y) a_{33} a_{32} + I_{xy} a_{31} a_{33} - I_{xz} a_{31} a_{32} + I_{yz} (a_{33}^2 - a_{32}^2) \right), \\ L_{Gy} &= \frac{3\mu}{r^3} \left((I_x - I_z) a_{31} a_{33} - I_{xy} a_{32} a_{33} + I_{xz} (a_{31}^2 - a_{33}^2) + I_{yz} a_{31} a_{32} \right), \\ L_{Gz} &= \frac{3\mu}{r^3} \left((I_y - I_x) a_{31} a_{32} + I_{xy} (a_{32}^2 - a_{31}^2) + I_{xz} a_{32} a_{33} - I_{yz} a_{31} a_{33} \right). \end{aligned}$$

Kinematic equations of space debris attitude motion can be found using transport theorem[14]

$$\frac{d\mathbf{e}_i}{dt} + \boldsymbol{\omega} \times \mathbf{e}_i = \boldsymbol{\omega}_b^{orb} \times \mathbf{e}_i, \quad i = 1, 2, 3 \quad (6)$$

where $\mathbf{e}_i = [a_{i1}, a_{i2}, a_{i3}]$ is the unit vector of the orbital frame in body frame components, $\boldsymbol{\omega}_b^{orb}$ is the angular velocity vector of the orbital frame relative to the inertial frame in body frame components. The vector $\boldsymbol{\omega}_b^{orb}$ can be found as $\boldsymbol{\omega}_b^{orb} = M_b^O \boldsymbol{\omega}_O^{orb}$, where $\boldsymbol{\omega}_O^{orb}$ has the following coordinates in the orbital frame:

$$\boldsymbol{\omega}_O^{orb} = \begin{bmatrix} \dot{\nu} \cos \lambda \sin \psi - \dot{\lambda} \cos \psi \\ \dot{\nu} \cos \lambda \cos \psi + \dot{\lambda} \sin \psi \\ \dot{\nu} \sin \lambda + \dot{\psi} \end{bmatrix}.$$

Equations (6) can be rewritten in the scalar form, taking into account $\mathbf{e}_1 = \mathbf{e}_2 \times \mathbf{e}_3$, $\mathbf{e}_2 = \mathbf{e}_3 \times \mathbf{e}_1$, $\mathbf{e}_3 = \mathbf{e}_1 \times \mathbf{e}_2$.

$$\begin{aligned}
\dot{a}_{11} &= \omega_z a_{12} - \omega_y a_{13} + (\dot{\psi} + \dot{\nu} \sin \lambda) a_{21} - (\dot{\nu} \cos \psi \cos \lambda + \dot{\lambda} \sin \psi) a_{31}, \\
\dot{a}_{12} &= \omega_x a_{13} - \omega_z a_{11} + (\dot{\psi} + \dot{\nu} \sin \lambda) a_{22} - (\dot{\nu} \cos \psi \cos \lambda + \dot{\lambda} \sin \psi) a_{32}, \\
\dot{a}_{13} &= \omega_y a_{11} - \omega_x a_{12} + (\dot{\psi} + \dot{\nu} \sin \lambda) a_{23} - (\dot{\nu} \cos \psi \cos \lambda + \dot{\lambda} \sin \psi) a_{33}, \\
\dot{a}_{21} &= \omega_z a_{22} - \omega_y a_{23} - (\dot{\psi} + \dot{\nu} \sin \lambda) a_{11} + (\dot{\nu} \sin \psi \cos \lambda - \dot{\lambda} \cos \psi) a_{31}, \\
\dot{a}_{22} &= \omega_x a_{23} - \omega_z a_{21} - (\dot{\psi} + \dot{\nu} \sin \lambda) a_{12} + (\dot{\nu} \sin \psi \cos \lambda - \dot{\lambda} \cos \psi) a_{32}, \\
\dot{a}_{23} &= \omega_y a_{21} - \omega_x a_{22} - (\dot{\psi} + \dot{\nu} \sin \lambda) a_{13} + (\dot{\nu} \sin \psi \cos \lambda - \dot{\lambda} \cos \psi) a_{33}, \\
\dot{a}_{31} &= \omega_z a_{32} - \omega_y a_{33} + (\dot{\nu} \cos \psi \cos \lambda + \dot{\lambda} \sin \psi) a_{11} + (\dot{\lambda} \cos \psi - \dot{\nu} \sin \psi \cos \lambda) a_{21}, \\
\dot{a}_{32} &= \omega_x a_{33} - \omega_z a_{31} + (\dot{\nu} \cos \psi \cos \lambda + \dot{\lambda} \sin \psi) a_{12} + (\dot{\lambda} \cos \psi - \dot{\nu} \sin \psi \cos \lambda) a_{22}, \\
\dot{a}_{33} &= \omega_y a_{31} - \omega_x a_{32} + (\dot{\nu} \cos \psi \cos \lambda + \dot{\lambda} \sin \psi) a_{13} + (\dot{\lambda} \cos \psi - \dot{\nu} \sin \psi \cos \lambda) a_{23}.
\end{aligned} \tag{7}$$

It should be noted that only six of the nine elements of the matrix of the direction cosines are independent. The coupling equations can be written in the form $\mathbf{e}_1 \cdot \mathbf{e}_2 = 0$.

Angle ψ could be found from the fact that the vector of the velocity $\mathbf{V}_C = \dot{\mathbf{r}}$ lies in the plane Cx_Oz_O . It follows that $\mathbf{V}_C \cdot \mathbf{e}_2 = 0$, and after translation of these vectors into the inertial frame we obtain

$$\psi = \arctan \left(\frac{\dot{\lambda}}{\dot{\nu} \cos \lambda} \right). \tag{8}$$

Differentiation of this equation gives

$$\dot{\psi} = \frac{\dot{\lambda}^2 \dot{\nu} \sin \lambda + \ddot{\lambda} \dot{\nu} \cos \lambda - \dot{\lambda} \ddot{\nu} \cos \lambda}{\dot{\lambda}^2 + \dot{\nu}^2 \cos^2 \lambda}. \tag{9}$$

The second derivatives can be found from (2).

The equations (2), (3), (7) form a closed system, describing the motion of the space debris in orbit, taking into account its rotation around the center of mass of the space debris.

2.2 Plane motion of the space debris

In the particular case of a plane motion of a dynamically symmetric space debris ($I_{xy} = I_{xz} = I_{yz} = 0$), the equations can be significantly simplified. In this case $\lambda = 0$, $\psi = 0$. Orientation of the body frame relative the orbital frame can be defined by one angle φ (Figure 2). Rotation matrix takes form:

$$\mathbf{M}_O^b = \begin{bmatrix} \cos \varphi & 0 & \sin \varphi \\ 0 & 1 & 0 \\ -\sin \varphi & 0 & \cos \varphi \end{bmatrix}$$

Equations of motion (2), (3) can be rewritten in simple form

$$\ddot{r} = \dot{v}^2 r - \frac{\mu}{r^2} + \frac{F_{Iz}}{m}, \quad \ddot{v} = -\frac{2\dot{v}\dot{r}}{r} + \frac{F_{Ix}}{rm}, \quad (10)$$

$$\ddot{\varphi} = \ddot{v} - \frac{3\mu(I_x - I_z) \sin \varphi \cos \varphi}{r^3 I_y} + \frac{L_{Iy}}{I_y}. \quad (11)$$

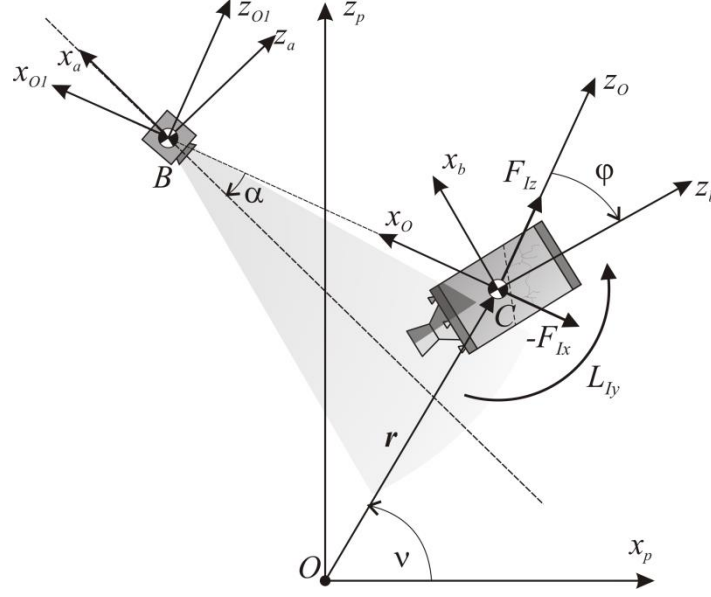


Figure 2: Plane motion of the system.

2.3 Method of the ion beam force and torque calculation

To calculate the ion flux force and torque let us use Newton's Impact Theory, which is based on the idea that pressure exerted on a surface with impinging flow is equal to the normal component of the momentum of the impinging particles [15]. This approach is successfully used for approximate calculation of aerodynamic characteristics of supersonic vehicles [16]. The surface of the body is divided into triangles. For each triangle inside the flow, the force acting on it can be calculated as

$$\mathbf{F}_j = -n_j m_0 V_j^2 \cos^2 \alpha_{sj} A_j \mathbf{N}_j, \quad (12)$$

where $\mathbf{V}_j = \left[-u_0, \frac{u_0 y_{aj}}{-x_{aj}}, \frac{u_0 z_{aj}}{-x_{aj}} \right]$ is the velocity of the ion flux at the point P_j , P_j is the barycenter of j -th triangle. This point has coordinates $[-x_{aj}, y_{aj}, z_{aj}]$ in the frame $Bx_a y_a z_a$, n_j is the plasma density at the point P_j [17]

$$n_j = \frac{n_0 R_0^2}{x_{aj}^2 \tan^2 \alpha_0} \exp\left(-\frac{3(y_{aj}^2 + z_{aj}^2)}{x_{aj}^2 \tan^2 \alpha_0}\right), \quad (13)$$

n_0 is the plasma density at the beginning of the far region, m_0 is the mass of particle, R_0 is the radius of the beam at the beginning of the far region, u_0 is the axial component of the ion flux velocity, α_0 is the divergence angle of the beam, α_{sj} is the angle between the velocity \mathbf{V}_j and the normal unit vector \mathbf{N}_j of the j -th triangle (Figure 3), A_j is the area of j -th triangle.

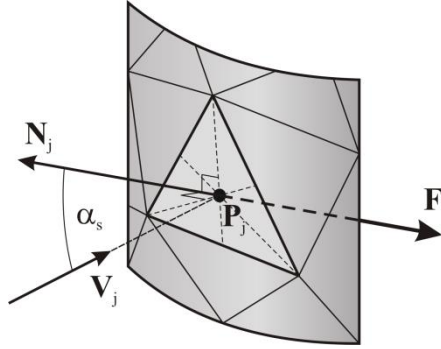


Figure 3: Force acting on j -th triangle.

The ion flux torque vector relative the space debris center of mass can be calculated as

$$\mathbf{L}_I = \sum_{j=1}^k \overline{CP}_j \times \mathbf{F}_j \quad (14)$$

where k denotes triangles inside the ion beam flow. The ion beam force is

$$\mathbf{F}_I = \sum_{j=1}^k \mathbf{F}_j. \quad (15)$$

The authors developed a program in Matlab that performs the calculation of (14) and (15).

3. Results and Discussion

Let us consider deorbiting of Cosmos 3M stage from the circular orbit of 500 km height. The stage is considered as a cylinder which center of mass lies on the axis and plane of symmetry. Parameters of the stage are given in Table 1. Table 2 contains parameters of electric-reactive engine. For calculation of ion beam force and torque the cylinder was divided into 54836 triangles.

Table 1: Space debris (Cosmos 3M) parameters

Parameter	Value
Mass m	1400 kg
Transversal moment of inertia I_x	6800 kg m ²

Transversal moment of inertia I_y	6800 kg m ²
Longitudinal moment of inertia I_z	1300 kg m ²
Products of inertia I_{xy}, I_{xz}, I_{yz}	0 kg m ²
Length	6.5 m
Radius	1.2 m

Table 2: Parameters for ion beam force and torque calculation

Parameter	Value
Plasma density n_0	$2.6 \cdot 10^{16} \text{ m}^{-3}$
Mass of particle (xenon) m_0	$2.18 \cdot 10^{-25}$
Radius of the beam at the beginning of the far region R_0	0.1 m
Axial component of the ion flux velocity u_0	38000 m/s
Divergence angle of the beam	15°
Distance between thruster exit and debris centre ρ_B	15 m

Let us consider plane motion of the system. Figures 4-6 show projections of (14) and (15) on the axis of orbital frame as functions of angle φ for various values of α , which defines ion beam axis direction. Let us investigate the influence of α on the force. Since the considered body is symmetric with respect to the plane $Cx_b y_b$, it suffices to consider only the positive values of the angle. The values for the negative angle can be obtained from the relations

$$F_{I_x}(-\alpha) = F_{I_x}(\pi - \alpha), \quad F_{I_z}(-\alpha) = -F_{I_z}(\pi - \alpha), \quad L_{I_y}(-\alpha) = -L_{I_y}(\pi - \alpha).$$

Figures 4 and 5 show that increasing the angle α leads to a decrease in the modules of F_{I_x} and F_{I_z} . It should be noted that even at an angle $\alpha = 1.87$ there is a partial blowing of the stage. At the angle $\alpha = 0$, the maximum F_I force is observed. Let us consider points A_k of the local maxima and minima of the curve $F_{I_x}(\varphi)$ (for $\alpha = 0$) on Figure 4. Figure 7 demonstrates positions of the Cosmos 3M stage corresponding to these points in the orbital frame. To estimate the time of the debris removal from the orbit, let us simulate motion of the system using equations (10) at a fixed angle φ . Table 3 contains results of simulations. The most effective is orientation of the stage over the angle $\varphi = \pi / 2$. In this case the time of descent to an altitude of 100 km is 120 days. At the least effective case $\varphi = 2.18 \text{ rad}$, the descent takes 288 days.

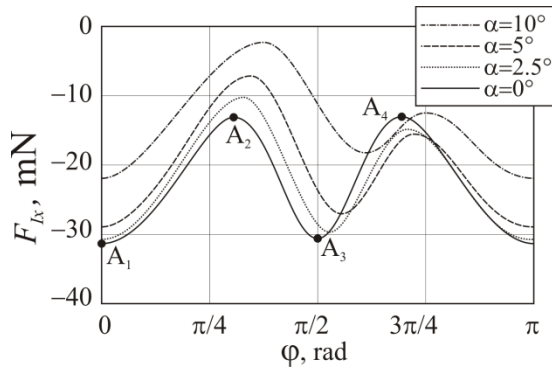


Figure 4: Dependence of ion beam force projection F_{Lx} on deflection angle φ .

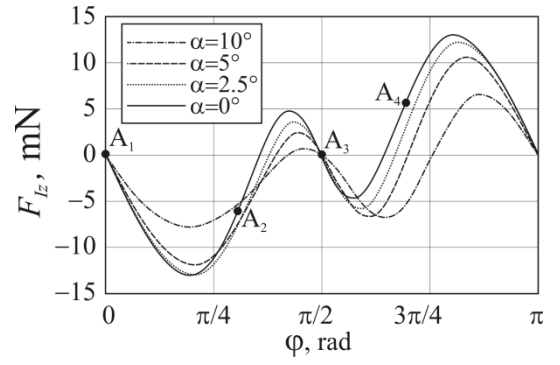


Figure 5: Dependence of ion beam force projection F_{Lz} on deflection angle φ .

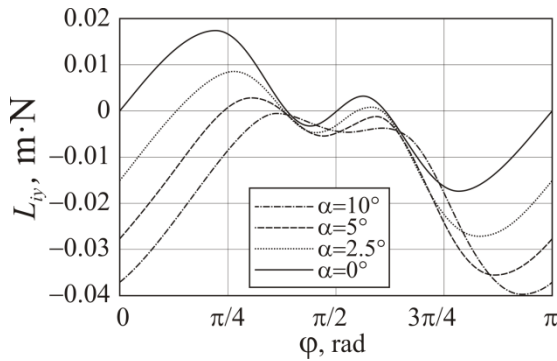


Figure 6: Dependence of ion flux torque projection L_{Ty} on deflection angle φ .

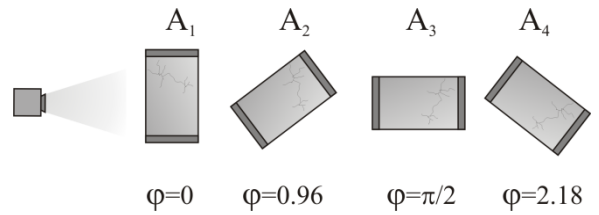


Figure 7: The positions of the Cosmos 3M stage.

The close effectiveness of the cases $\varphi = 0$ and $\varphi = \pi/2$ is easily explained. Despite the fact that the surface area blown by the ion flow is larger in the first case, the modulus of the force acting on each small section of this surface is less due to the orientation of this section (Figure 8).

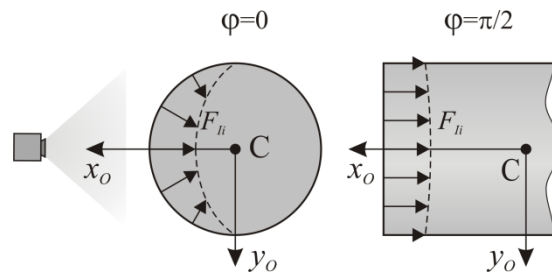


Figure 8: Comparison of cases when $\varphi = 0$ and $\varphi = \pi/2$.

It should be noted that force F_{Lz} takes values of the same order with F_{Lx} (Figures 4 and 5). By analogy with the case of motion in the atmosphere, we can talk about the presence of a lift force that will move the considered cylinder from the ion beam axis. In this regard, additional efforts should be taken to control the active spacecraft position and orientation. This question

remains behind the scopes of this study, since in the developed models the position of the active spacecraft \mathbf{p}_B is invariant in the orbital coordinate system $Cx_oy_oz_o$.

Table 3: Time of the debris removal from 500 km to 100 km altitude

Case	φ_0	$\dot{\varphi}_0$	F_{I_x}	F_{I_z}	Time
Fixed orientation A ₁	0	0	-0.0313 N	0	120 days
Fixed orientation A ₂	0.96	0	-0.0131 N	-0.0061 N	287 days
Fixed orientation A ₃	$\pi / 2$	0	-0.0306 N	0	123 days
Fixed orientation A ₄	2.18	0	-0.0130 N	0.0062 N	288 days
Oscillations	1.47	0			180 days
Oscillations	1.67	0			181 days
Oscillations	1.01	0			286 days
Oscillations	2.13	0			287 days
Rotation	0	0.015rad/s			229 days

In order to analyze the motion of the cylinder relative to its center of mass, let us consider Figure 6. Three types of graphs are observed: when function $L_y(\varphi)$ has five roots (for example $\alpha = 0$ on figure 6), when it has two roots (for example $\alpha = 5^\circ$ on figure 6) or when it has no roots (for example $\alpha = 10^\circ$ on figure 6). As the gravity gradient torque acts in addition to the ion beam torque, their ratio determines the form of the phase portrait of the equation (11). A series of numerical calculations showed that one of three types of phase portrait can be realized. If resultant moment has five roots, there are three saddle points and two centers (Figure 9). The phase portrait contains three oscillation areas. This case can exist only for $\alpha = 0^\circ$. If resultant moment has four roots, there are two saddle points and two centers (Figure 10). The phase portrait contains two oscillation areas. If resultant moment has two roots, there are one saddle point and one center (Figure 11). The phase portrait contains one oscillation area.

Figures 10 and 11 allow to conclude that if at the initial time the space debris rotates in the direction corresponding to the upper part of the phase portrait, then as a result of the action of the ion flow the rotation will first slow down, and then will spin-up in the opposite direction.

It should be noted, that the centers in the phase portraits are located close to the minimum points on the curve F_{I_x} , and the saddle points are located close to maximum points on this curve. In this regard, it can be concluded that the removal of space debris in the regime of oscillations near stable equilibrium positions is ineffective. It makes sense to develop control laws for angle

α , which provide stabilization of the cylindrical space debris near the saddle point. This topic will be the subject of further research.

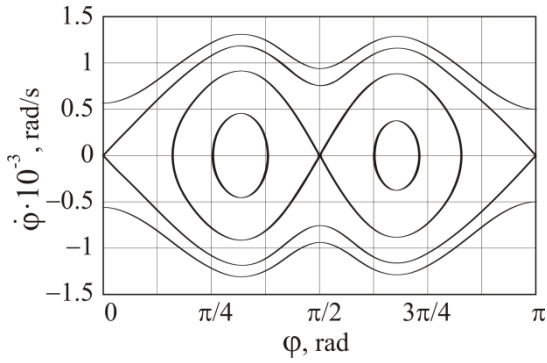


Figure 9: Phase portrait for case 1 ($\alpha = 0$)

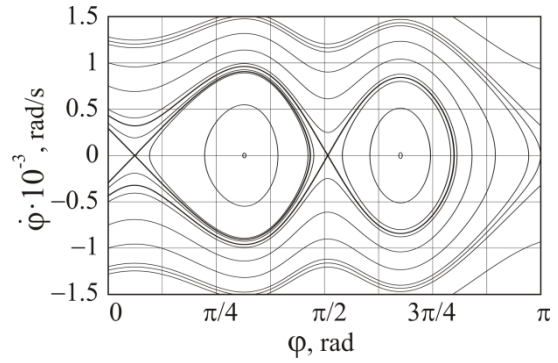


Figure 10: Phase portrait for case 2 ($\alpha = 0.5^\circ$)

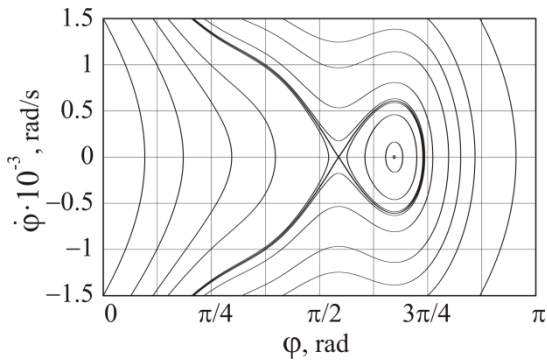


Figure 11: Phase portrait for case 3 ($\alpha = 5^\circ$)

These phase portraits were plotted on a relatively short time interval (about 3 hours). On this interval the change in the altitude of the orbit is insignificant. During the process of the space debris deorbiting, the magnitude of the gravity gradient torque will slowly increase and the phase portraits will deform.

Conclusions

The non-contact method of the space debris deorbiting by an active spacecraft with ion thrusters was considered in this paper. This is a relatively new method of space debris removal, which main advantage is no need for complex and dangerous docking stage. The mathematical models developed within the framework of the article allow to study the attitude motion of space debris under the influence of the ion beam on the orbit. Calculation of ion beam force and torque was performed using Newton Impact theory. It was showed that motion of the space debris around its center of mass has a significant effect on its removal time. For the case of plane motion, phase portraits describing the motion of the space debris relative its center of mass were

constructed. Comparison of the descent times in different motion modes was carried out. It was shown that descent in modes where the space debris oscillates in a small neighborhood of stable equilibrium positions is ineffective in terms of descent time. The results can be used to create new effective systems of large space debris removal.

Conflicts of Interest

The authors declare that they have no conflicts of interest regarding this research article.

Acknowledgments

This study was supported by the Russian Science Foundation (Project No. 17-79-20045).

References

- [1] Reed J., Barraclough S., "Development of harpoon system for capturing space debris," ESA Special Publication, vol. 723, 8 pages, 2013.
- [2] Guang Zhai, Jing-ru Zhang, Zhang Yao, "Circular Orbit Target Capture Using Space Tether-Net System," *Mathematical Problems in Engineering*, vol. 2013, Article ID 601482, 11 pages, 2013. doi:10.1155/2013/601482
- [3] Aslanov V., Yudinsev V. "Dynamics of large space debris removal using tethered space tug," *Acta Astronautica*, vol. 91, pp. 149-156, 2013 doi: 10.1016/j.actaastro.2013.05.020
- [4] Kuroda S., Higuchi T., Tsujimoto Y., Ueno S., "Capturing simulation of space debris with super multi-link space manipulator," 2016 55th Annual Conference of the Society of Instrument and Control Engineers of Japan (SICE), Tsukuba, pp. 660-666, 2016. doi: 10.1109/SICE.2016.7749278
- [5] Shan M., Guo J., Gill E. "Review and comparison of active space debris capturing and removal methods," *Progress in Aerospace Sciences*, vol. 80, pp. 18-32, 2016. doi: 10.1016/j.paerosci.2015.11.001
- [6] Hogan E. A., Schaub H., "Space debris reorbiting using electrostatic actuation," *Advances in the Astronautical Sciences*, vol. 144, pp. 73-92. 2012.
- [7] Bombardelli C., Pelaez J, "Ion Beam Shepherd for Contactless Space Debris Removal," *Journal of Guidance, Control, and Dynamics*, vol. 34, no. 3, pp. 916-920, 2011. doi : 10.2514/1.51832
- [8] Ishkov S.A., Filippov G.A., "A disposal of the space debris with special spacecraft debris collector using low trust," *Engineering Letters*, vol 23, issue 2, pp. 98-109, 2015.

- [9] Alpatov A., Cichocki F., Fokov A., Khoroshylov S., Merino M., Zakrzhevskii A., "Determination of the force transmitted by an ion thruster plasma plume to an orbital object," *Acta Astronautica*, vol. 119, pp. 241-251, 2016. doi: 10.1016/j.actaastro.2015.11.020
- [10] Nadiradze A.B., Obukhov V.A., Pokryshkin A.I., Popov G.A., Svotina V.V., "Modeling of the ion beam force impact and erosive action on a large-sized object of technogenic space debris," *Proceedings of the Russian Academy of Sciences. Power Engineering*, no 2, pp. 146-157, 2016.
- [11] Cichocki F., Merino M., Ahedo E., Smirnova M., Mingo A., Dobkevicius M., "Electric Propulsion Subsystem Optimization for "Ion Beam Shepherd" Missions," *Journal of Propulsion and Power*, vol. 33, no. 2, pp. 370-378, 2017. doi: 10.2514/1.B36105
- [12] Alpatov A.P., Zakrzhevskii A.E., Fokov A.A., Khoroshylov S.V., "Determination of Optimal Position of 'Ion Beam Shepherd' with Respect to Space Debris Object," *Technical Mechanics*, no. 2, pp. 37– 48, 2015. <http://dspace.nbuv.gov.ua/handle/123456789/88531>
- [13] Schaub, H., and Junkins, J. L., "Analytical mechanics of aerospace systems," 2nd ed., Reston, VA, 2009, Chaps. 4.
- [14] Likins, P. W., "Elements of Engineering Mechanics," McGraw-Hill, New York, 1973.
- [15] Jaslow, H., "Aerodynamic Relationships Inherent in Newtonian Impact Theory," *AIAA Journal*, vol. 6, no. 4, 1968, pp. 608–612. doi:10.2514/3.4552
- [16] V. Aslanov, A. Ledkov, "Chaotic Motion of a Reentry Capsule During Descent into the Atmosphere," *Journal of Guidance, Control, and Dynamics*, vol. 39, no. 8, pp. 1834-1843, 2016. doi: 10.2514/1.G000411
- [17] A.P. Alpatov, A.A. Fokov, S.V. Khoroshylov, A.P. Savchuk, "Error Analysis of Method for Calculation of Non-Contact Impact on Space Debris from Ion Thruster," *Mechanics, Materials Science & Engineering Journal*, 2016, 13 pages, doi: 10.13140/RG.2.1.3986.1361